

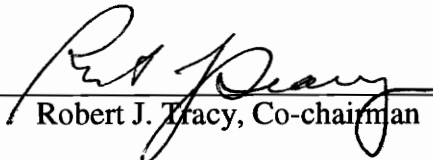
**PETROGENESIS AND GEOCHEMISTRY OF KYANITE-BEARING
PEGMATITES IN THE BUNCOMBE PEGMATITE DISTRICT,
NORTH CAROLINA**

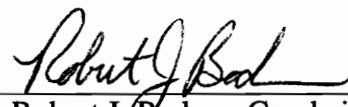
by

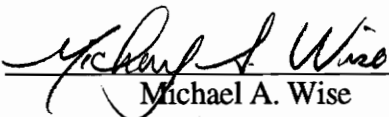
Keith Yates Wood

Thesis submitted to the Faculty of the
Virginia Polytechnic Institute and State University
in partial fulfillment of the requirements for the degree of
MASTER OF SCIENCE
IN
GEOLOGY

APPROVED:


Robert J. Tracy, Co-chairman


Robert J. Bodnar, Co-chairman


Michael A. Wise

August, 1996

Blacksburg, Virginia

Keywords: Pegmatite, Kyanite, Magmatic, Biotite

LD
5655
V855
1996
W663
c.2

**Petrogenesis and Geochemistry of Kyanite-Bearing
Pegmatites in the Buncombe Pegmatite District,
North Carolina**

by

Keith Yates Wood

Robert J. Tracy and Robert J. Bodnar, Co-Chairmen

Department of Geological Sciences

(ABSTRACT)

Kyanite is generally considered to be a product of metamorphism. This study investigates a set of kyanite-bearing pegmatites that represent a case in which kyanite crystallized directly from melt. The pegmatites intrude spinel orthopyroxene hornblendite in the Buncombe Pegmatite District in the Eastern Blue Ridge of North Carolina. One site was studied in detail and survey studies of two other occurrences were made. The pegmatites contain quartz, large euhedral crystals of plagioclase, biotite, and kyanite, as well as apatite, muscovite, tourmaline, and microscopic primary sillimanite. Potassium feldspar is notably absent. One site, the Thomas Mine, was examined in detail in order to determine the mode of occurrence for these rocks. Excavation revealed pegmatite with two texturally and mineralogically distinct zones. Biotite-rich rocks surrounding the pegmatite indicate strongly potassic alteration of the host hornblendite.

Trace element data obtained for kyanite and biotite from the pegmatite show clear patterns related to chemical fractionation of these components during crystallization. Major element geochemistry of the pegmatite and host rocks are consistent with magmatic intrusion. Reaction of the pegmatite melt

with the host rocks led to the formation of large amounts of biotite, and depleted the melt in potassium. The remaining melt became saturated in aluminum silicate and crystallized kyanite and sillimanite. Wallrock assemblages, fluid inclusions in pegmatite quartz, the coexistence of kyanite and sillimanite as primary phases, and geothermobarometry on nearby unaltered rocks all indicate conditions of formation of approximately 600-800 MPa and 625-675°C, near those of peak metamorphism for the region.

Dedication

This thesis is dedicated to my father, Richard Wood. His courage and integrity are more of an inspiration to me every day. Keep holding on to Him, Dad. I love you so much.

Acknowledgments

Many thanks go to my excellent wife, Patricia, for encouragement, assistance, and more than her share of help with the more laborious aspects of my field work, specifically the digging of a large hole in the ground. Thanks also go to Bob Tracy for his petrologic insight and for being an all-around great advisor. Bob Bodnar offered much assistance and sage advice, frequently on short notice, for which I am thankful. Mike Wise ran a great pegmatite Field Camp in Maine that was immensely helpful, and also ran the XRF for my analyses. What a guy! Todd Solberg's help with the microprobe is also deeply appreciated. A debt of gratitude is also owed to the personnel of the National Park Service, who, I'm afraid, got more than they bargained for in this study. Frank Roth at the National Forest Service was tremendously helpful in allowing access to one of the sites studied here. Thanks also go to my parents for their support and encouragement. Greatest thanks and eternal gratitude go to God and His living Son, Jesus Christ. How could I even begin to count His kindnesses? And, of course, where would any of us be without the mineral kingdom? Thanks, all of you.

TABLE OF CONTENTS

Abstract	ii
Dedication	iv
Acknowledgments	v
List of Figures	vii
List of Tables	viii
Introduction	1
Previous Work	1
Geologic Setting	4
Petrography	23
Chemical Analyses	24
XRF Data	25
Microprobe Data	28
Fluid Inclusions	28
Discussion	30
P-T Conditions of Formation	41
Undercooling by Elevation of the Liquidus	47
Implications for Muscovite Class Pegmatites	50
Conclusion	52
References	53
Vita	56

LIST OF FIGURES

Figure 1	Map of Buncombe pegmatite district	5
Figure 2.	Photo of north end of pegmatite	8
Figure 3.	Photo of south end of pegmatite	10
Figure 4.	Close-up photo of kyanite crystal showing scallop texture	13
Figure 5.	Photos of pegmatite sample from core	16
	A. Large plagioclase, quartz, and kyanite	17
	B. Kyanite with tourmaline prism	18
	C. Giant kyanite with tourmaline	20
Figure 6.	Th-Tm diagram showing fluid inclusion data	32
Figure 7.	Trace element levels in biotite	33
Figure 8.	Cartoon pegmatite map showing locations of samples	34
Figure 9.	Paragenesis of minerals in the pegmatite	37
Figure 10.	P-T diagram showing CO ₂ isochores	42
Figure 11.	P-T diagram showing thermobarometric equilibria	45
Figure 12.	Distribution of garnet-biotite temperatures	46
Figure 13.	Yoder's ternary phase diagram for system Ab-An-Qtz-H ₂ O	49

LIST OF TABLES

Table 1.	Trace-element analyses	26
Table 2.	Whole-rock analyses	27
Table 3.	Thomas mine mineral analyses	29
Table 4.	Pelitic schist mineral analyses	44

**Petrogenesis and Geochemistry of Kyanite-Bearing
Pegmatites in the Buncombe Pegmatite District,
North Carolina**

Introduction

Kyanite-bearing veins and segregations of many types have been discussed at length in the literature. Many of these rocks consist only of quartz and kyanite (Read 1932, Miyashiro 1951, Sauniac and Touret 1983, many others) although staurolite, paragonite (Keller 1968), plagioclase (Stuckey 1935), tourmaline (Keller 1968), muscovite, and biotite have also been reported. Although a magmatic origin has been suggested for some kyanite deposits (Stuckey 1935, Temperly 1953, Banerji 1954, Nordstrom 1947, Heinrich 1949, Heinrich 1950) none of these studies presents conclusive evidence for this origin. This study presents geologic and geochemical data on an unusual kyanite-bearing pegmatite deposit in the Buncombe Pegmatite District of North Carolina. The deposit represents a significant departure from the granite minimum composition typical of most pegmatites. The data on this deposit represent the first clear evidence for a magmatic origin for kyanite-bearing pegmatites.

Previous Work

The term pegmatite has been used by some to refer to coarse-grained rocks regardless of origin, whereas others use the term to refer only to coarsely crystalline granitic (*sensu lato*) rocks specifically of igneous origin.

The meaning intended by the authors of earlier studies is in some cases unclear. Therefore, studies in which kyanite-bearing rocks are referred to as pegmatites, or in which a magmatic origin is proposed for kyanite deposits, are reviewed below.

Before the discovery of the deposits studied in this work, Stuckey (1935) suggested that coarsely crystalline kyanite segregations in North Carolina originated from escaping solutions from pegmatitic and granitic magmas. Although most of the larger deposits he examined are associated with granitoids in the Spruce Pine pegmatite district, many others are far removed from granitoids of any significance. Temperly (1953) used the term pegmatite to indicate those deposits that contain feldspar in addition to kyanite and quartz in his study of kyanite deposits in Kenya.

Banerji (1954) proposed a magmatic origin for a complexly mineralized kyanite deposit, which he referred to as a pegmatite, lying along a fault in quartzite in the Singhbhum district, Bihar, India. Mica schists occur nearby. The deposit is described as a vein having a core composed of massive kyanite. The rocks also contain staurolite, topaz, tourmaline, and dumortierite. Banerji asserted that the kyanite and staurolite, along with feldspar and quartz, were of magmatic origin based on the dike-like structure of the rocks and apparent zoning within them. Banerji related the rocks to a nearby granite, and further states that formation of this deposit was followed by other stages of mineralization. However, the existence of a melt so rich in aluminum as to produce a core of massive kyanite seems unlikely in the light of data from experimental petrology. Banerji's case for a magmatic origin also appears weak in view of the rather restricted range in composition commonly observed in igneous rocks. Nonetheless it is possible that boron-rich fluids

(not necessarily melt) derived from the nearby Singhbhum granite could have been involved, especially if boron aids in the transport of aluminum.

Heinrich (1950) mentioned a kyanite- and staurolite-bearing pegmatite hosted by biotite gneiss near a rhodolite garnet deposit in western North Carolina. Heinrich inferred an igneous origin but did not present quantitative chemical data to support this conclusion. It is noteworthy that the nearby rhodolite deposit, like the pegmatites examined in this study, occurs in metamorphosed ultramafic rocks. The kyanite-bearing rocks there occur within seventy meters of the rhodolite deposit. The mineral assemblage in the Ennis, Montana, kyanite deposits (Nordstrom 1947, Heinrich 1949) is remarkably similar to that of the rocks in this study but also includes microcline. Quartz is reported to make up as much as 75% of some outcrops. Heinrich (1949) referred to these rocks as pegmatites and suggested a magmatic origin, postulating the intrusion of highly peraluminous pegmatite-forming magmas into the mafic and pelitic schists of the area. However, the existence of such silica- and alumina-rich magmas is improbable because of the prohibitively high temperatures necessary to generate them. Černý (1982) briefly mentioned several Russian studies reporting kyanite as a wall zone or border zone phase in pegmatites intruding kyanite-bearing rocks. It is unclear whether the kyanite crystallized directly from a pegmatite melt or was derived from the wallrocks. Černý (1982) discussed other Russian work, including a report of andalusite paramorphous after kyanite, but their nature remains obscure. Most of these rocks are reported to be directly associated with kyanite- or mica-schists.

Many of the studies discussed here are relatively old and predate not only modern geochemical methods but also the wealth of data available from

experimental petrology. Data in some of these studies may be consistent with a magmatic origin for kyanite, but other interpretations seem more plausible. Cases in which the reported mineral proportions seem far from bulk compositions of melts generated in experimental work appear particularly weak. Consequently, no strong case for kyanite of igneous origin appears to exist.

Geologic Setting

The Buncombe pegmatite district (Fig. 1) in the Blue Ridge of North Carolina lies about fifty kilometers west-southwest of the well-known Spruce Pine pegmatite district. The district surrounds Asheville, NC and is characterized by small, widely scattered, mineralogically simple pegmatites. Approximately ninety documented mica mines exist within the district (Lesure 1968) and there are probably as many more undocumented prospects. The largest pegmatites seldom exceed 100 meters in length, most being much smaller. The pegmatites generally contain two feldspars, quartz, and moderate amounts of muscovite. Plagioclase is typically the dominant feldspar. Rare accessory minerals include garnet, biotite, apatite, tourmaline, and beryl. Simple pegmatite mineralogy and kyanite to sillimanite grade host rocks suggest that these pegmatites belong to the muscovite class of Černý (1982, 1991).

Three unusual, K-feldspar-free, kyanite-bearing pegmatites within the Buncombe district have been studied to determine their origin (Wood 1995). The pegmatites intrude hornblendites in the Craggy Mountains of Buncombe County, part of the Ashe Metamorphic Suite (Abbott and Raymond 1984), near

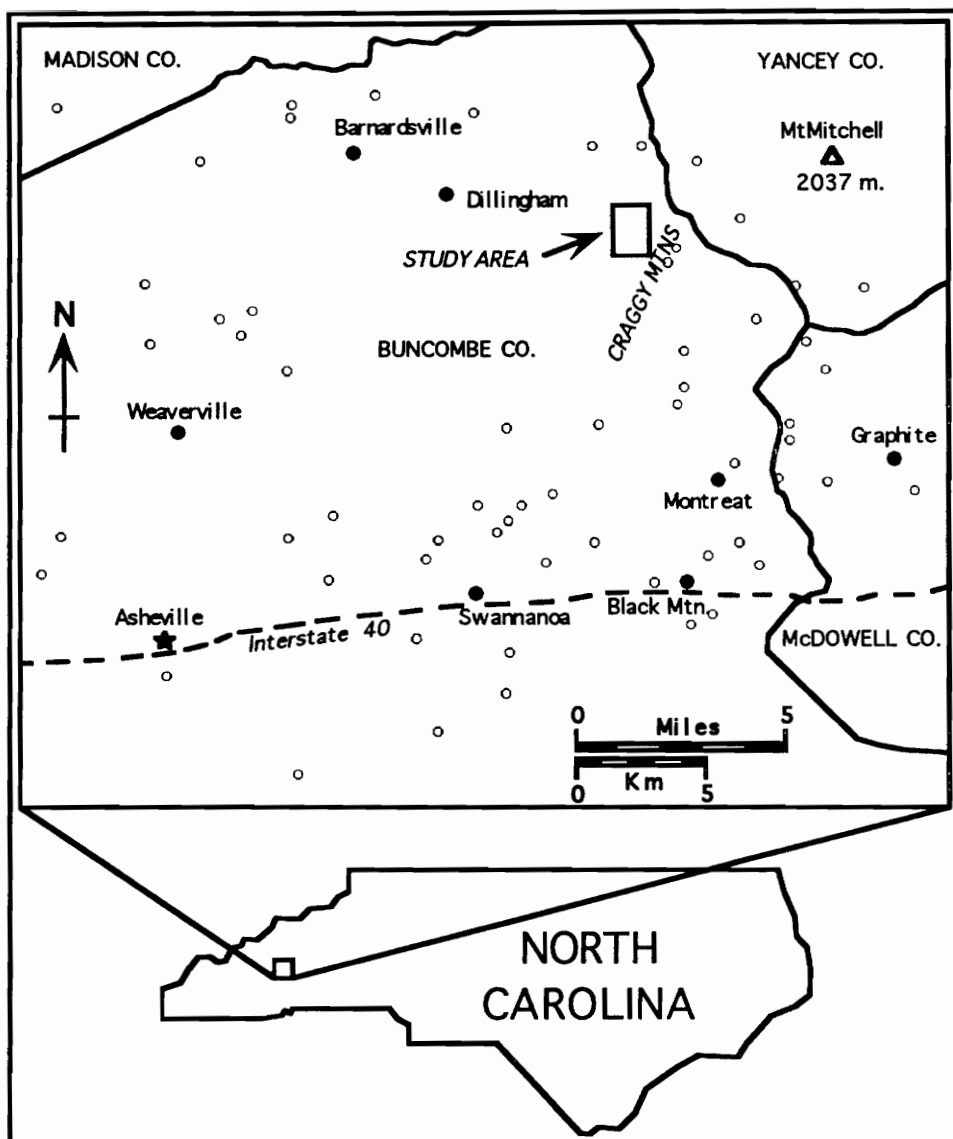


Fig. 1. Map showing a portion of the Buncombe pegmatite district (after Lesure 1968), principle towns, Interstate Highway 40, and the study area containing the Thomas and Meeper Mines and the Swan Prospect. Precise locations for these deposits are not given by request of the National Park Service. Small open circles represent known mica-bearing pegmatite deposits. These correspond with Lesure's (1968) map of muscovite deposits and are included to show the wide distribution of pegmatites in the Buncombe district.

the northeastern corner of the Buncombe district. Lesure *et al* (1982) described the Craggy Mountains as being composed largely of kyanite and sillimanite schists and gneisses and a few amphibolite layers. Lesure *et al* (1982) briefly described the Thomas Mine, one of the three similar deposits studied here, in their section on kyanite resources.

The three kyanite-bearing pegmatites are mineralogically similar, intrude similar host rocks, and occur within two kilometers of each other. A detailed study of one deposit, the Thomas Mine, and survey studies of two other sites, now named the Meeper Mine and the Swan Prospect, were conducted. The Thomas Mine consists of two pegmatite bodies ten meters apart in which the mineralogy is essentially identical. The pegmatites are hosted by hornblendite which in turn is within 20 meters of kyanite- and sillimanite-bearing schists. At each of the other two kyanite deposits, the contact of the hornblendites with the nearest schist is within less than 100 m of the pegmatite outcrops. Of the two pegmatite outcrops making up the Thomas mine, the western body is the smaller (5 m long and 1.5 m wide) whereas the eastern body is 10 m long and up to 2 m wide. Both have been extensively disturbed by mineral collectors. Excavation of backfill covering the larger eastern body exposed the northern and southern portions of the pegmatite, the center having been previously excavated to an unknown depth. The observed assemblages are described below in order of their occurrence starting from the unaltered host rocks and moving inward toward the core of the pegmatite.

The host rock for the Thomas Mine is weakly foliated olivine-bearing spinel-orthopyroxene-hornblendite containing trace amounts of ilmenite, euhedral chlorite, pyrrhotite, chalcopyrite and pentlandite. The contact of the hornblendite with a nearby kyanite- and sillimanite-bearing schist is twenty

meters northeast of the pegmatite. The first sign of pegmatite-related alteration is marked by the transition to the assemblage hornblende plus garnet with minor plagioclase. Adjacent to this are rocks containing hornblende and garnet with minor plagioclase and biotite, plus or minus quartz. Still further inward hornblende decreases significantly, giving way to biotite and garnet with minor quartz and plagioclase. Transitional rocks containing roughly equal proportions of biotite and hornblende exist but are uncommon. In some of the wallrocks garnet is absent and biotite is accompanied instead by gedrite and cummingtonite, with minor quartz and plagioclase. The garnet-biotite facies in some places marks the transition from melanocratic rocks to the leucocratic rocks of the pegmatite, whereas in other places, thick masses of biotite alone make up the margin of the pegmatite. The extent of alteration varies dramatically from one part of the margin to another. In some portions of the outcrop, nearly unaltered host rock is within a few centimeters of leucocratic pegmatite, whereas other portions exhibit nearly the complete spectrum of alteration facies spanning several tens of centimeters, commonly being dominated by garnet and hornblende with minor biotite. These assemblages are similar to those observed by Sanford (1982) along contacts where ultramafic rocks and adjacent schists have undergone metasomatic reactions accompanying amphibolite facies regional metamorphism.

The leucocratic rocks observed consist of a narrow (40-50 cm) northern portion (Fig. 2) and a wider (80-90 cm) southern portion (Fig. 3) separated by a wide center (2 m) which has been removed by collectors. The depth of the previous mining and the presence of several loose boulders in the backfill prevented *in situ* examination of the central parts of the pegmatite. The




Fig. 2. Photo of north end of pegmatite exposed at the Thomas Mine. Note masses of biotite containing kyanite crystals. Wallrock at top and bottom of photo (east and west sides, respectively) is almost pristine unaltered host rock. Rock hammer for scale.



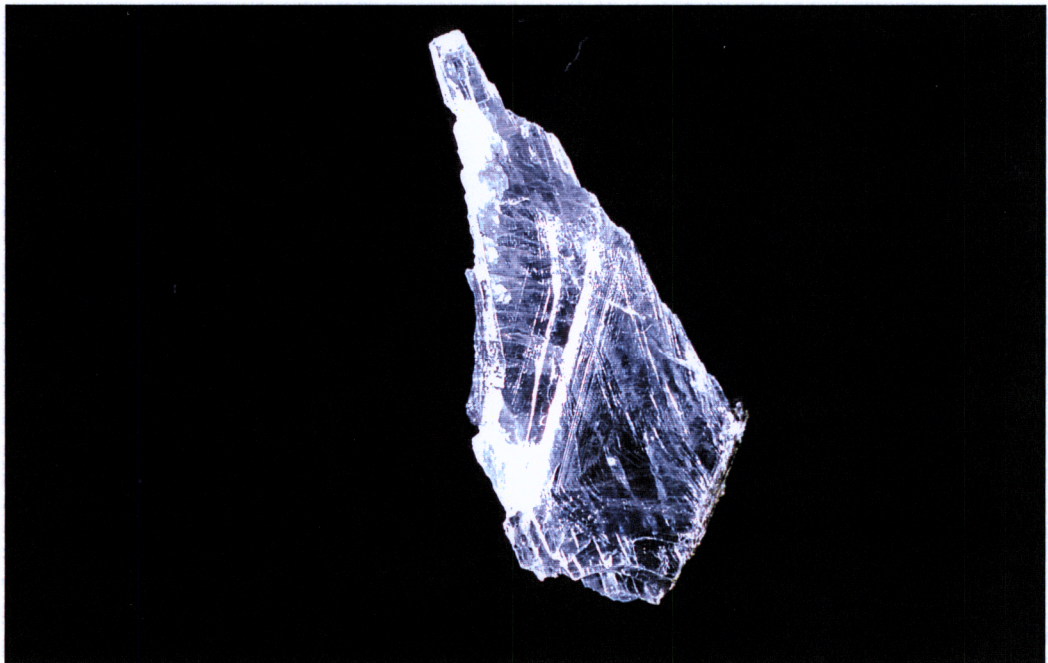
Fig. 3. Photo of south end of pegmatite exposed at the Thomas Mine. East is to the top of the photo. Note comparatively well-developed internal structure as compared with the north end shown in Fig. 2. Linear features are in most cases kyanite crystals. Note quartz-rich area on right containing glassy smoky quartz and little plagioclase. The immediate eastern wallrocks (top) consist of massive, matted biotite, visible as many white reflections on a dark background. Garnet-biotite rock makes up the eastern margin bordering the leucocratic rocks. The western border (bottom) is a sharp contact with nearly unaltered country rock, though further south (right, not shown) a large volume of the wallrocks consists of garnet-hornblende rock. The black area dividing the pegmatite near the middle of the photo is leucocratic rock stained with manganese oxides. Rock hammer for scale.



northern end consists of inhomogeneous rocks dominated by medium- to coarse-grained quartz and plagioclase and containing varying amounts of fine- to coarse-grained subhedral to euhedral biotite. Kyanite here is sparsely and erratically distributed, mainly as subhedral blades interlocked with books of biotite. Apatite is particularly common as euhedral green crystals up to 1 cm in the biotite masses, but occurs elsewhere as well. Garnet crystals averaging 0.5 cm are also common in the biotite.

The southern exposure (Fig. 3) revealed well-developed pegmatite with a consistent biotite-garnet margin several cm wide on the east and a very abrupt gradation from biotite to nearly unaltered host rock on the west. The pegmatite consists of subhedral to euhedral plagioclase crystals grading upward in size (to 10 cm) toward the center, together with equal amounts of anhedral quartz. Kyanite is present as large highly modified euhedral crystals up to 30 cm long by 4 cm wide by 1 cm thick. The kyanite crystals, making up perhaps 4% of the rock, are surrounded exclusively by blebs of quartz, and are of an aquamarine color with patchy dark blue color zoning in their centers. Modification of the kyanite crystals takes the form of scalloped terrace patterns not strongly controlled by the more common forms (Fig. 4). Biotite and apatite occur as isolated crystals in quartz and plagioclase. Accessory minerals observed include garnet, a single euhedral allanite crystal, and one 2mm grain of yellow uranium hydroxide (gummite). A quartz-rich area approximately 15 cm across is present near the middle of the exposure. This quartz is more transparent than quartz in other parts of the southern end, contains kyanite crystals similar to those nearby, and contains less biotite. All the rock of the northern and southern ends of the pegmatite exposure

Fig. 4. Detail of a single kyanite crystal from the outer zone showing scalloped morphology. Crystal is 3cm long. Diagonal line across crystal is a ridge separating two opposite-facing depressions. Many concentric terraces are present on either side of the dividing ridge. Irregular right edge of crystal is natural and exhibits similar complex morphology. C-axis is parallel to the length of the crystal.

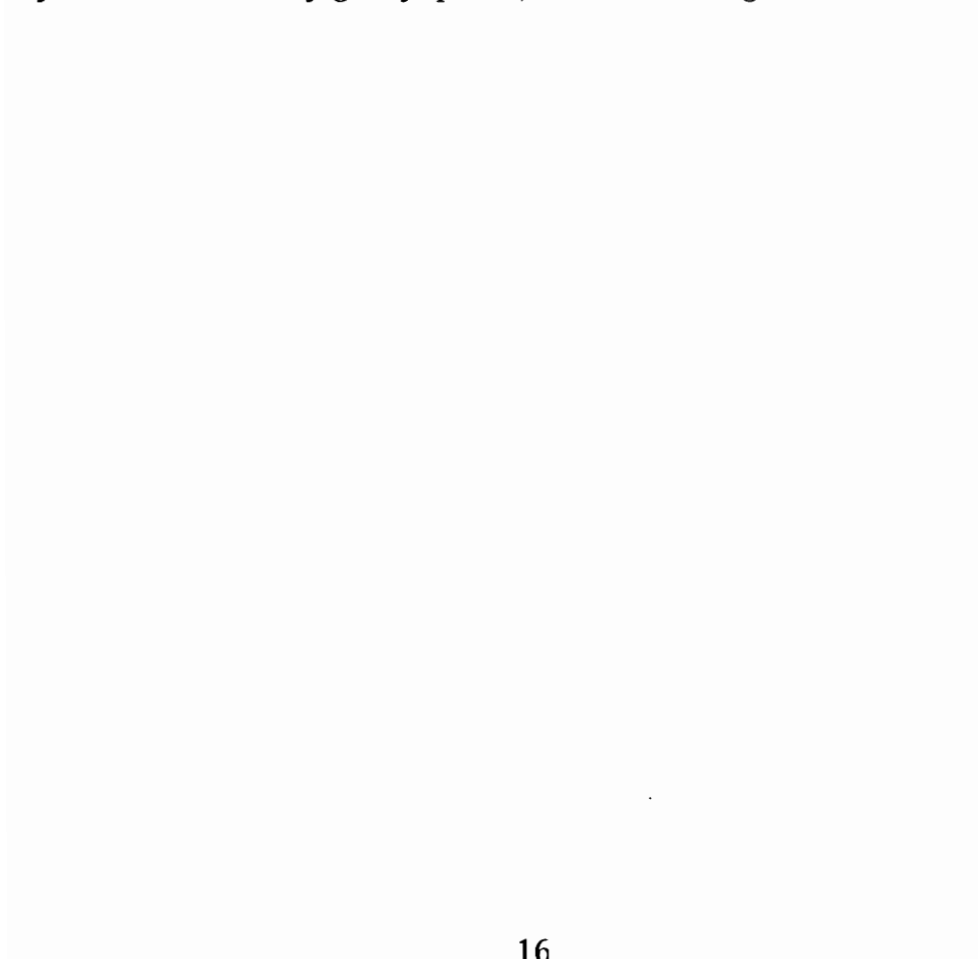


represents the outer zone of the pegmatite. K-feldspar is conspicuously absent from all the leucocratic rocks.

The missing central portion of the deposit clearly contained the core of the pegmatite. The following description of the texture of the core is based on abundant float at the site, specimens in local collections, and interviews with local collectors. The rocks consist of large (10-25 cm) blocky plagioclase crystals (Fig. 5a), masses of glassy quartz, and very dark brown prismatic tourmaline crystals up to 10 cm in length (Fig. 5b). Kyanite crystals reach lengths of 70 cm, widths of 10 cm, and are up to 2.5 cm thick (Fig. 5c). Kyanite crystals in this zone lack the terrace modifications present in the outer zone. Tourmaline crystals up to 8 cm in length are commonly densely clustered around kyanite crystals, but occur singly and in radiating clusters as well. Muscovite as thin books up to 5 cm across is restricted to this zone. Euhedral allanite, rutile and xenotime are trace accessory phases. Biotite is rare. The kyanite generally lacks the aquamarine color of the outer zone, with some portions of crystals being nearly or completely colorless, or tinted a faint green. Nonetheless, dark blue patches similar to those in kyanites of the outer zone are common. No K-feldspar is present in any of the rocks at the Thomas Mine.

A survey study of the two other sites revealed striking similarities in mineralogy and field relations. The Swan prospect, located 100 m south of the Thomas mine, is not currently exposed, but abundant tailings revealed that quartz, plagioclase, muscovite, and biotite are the main minerals. Muscovite is abundant as large subhedral to euhedral books, and is more common than biotite in the float. Tourmaline was observed as euhedral to anhedral crystals, in all sizes up to 10 cm in diameter and 20 cm in length. The tourmaline

Fig. 5. Three photos from a single specimen of pegmatite inner zone rock showing characteristic features: 5a: Large euhedral plagioclase crystal surrounded by glassy quartz, both containing tourmaline.



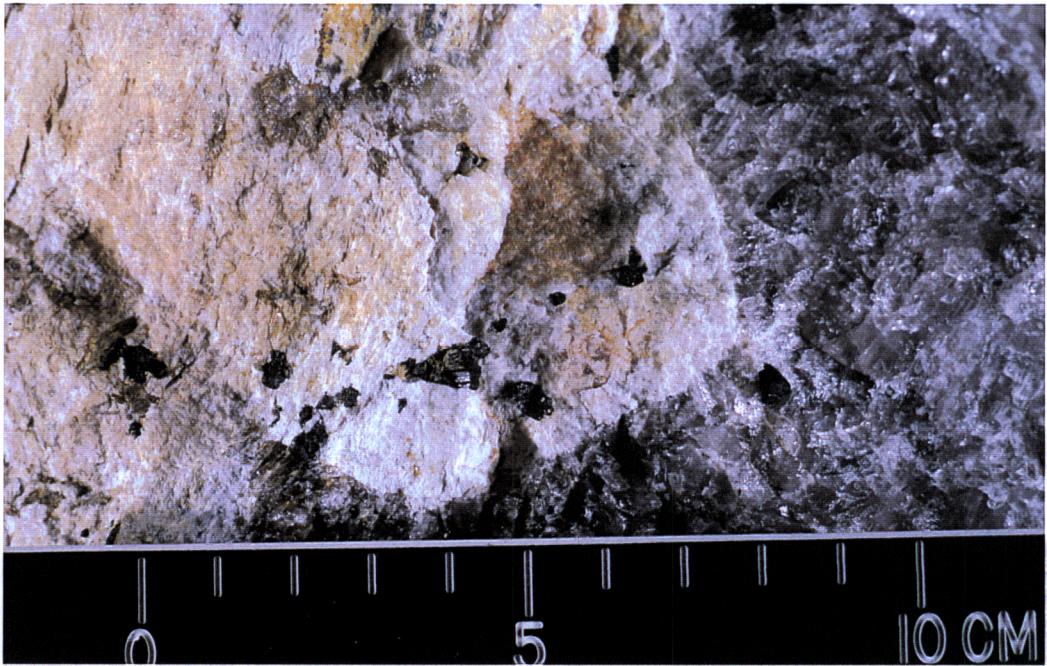


Fig. 5b: Single 6cm tourmaline in quartz. Many small tourmaline crystals occur below the single prism and are clustered next to the thick kyanite crystal. The kyanite is viewed edgewise and cuts diagonally across the lower right portion of the photo. Plagioclase is adjacent to the kyanite opposite the quartz and tourmaline.




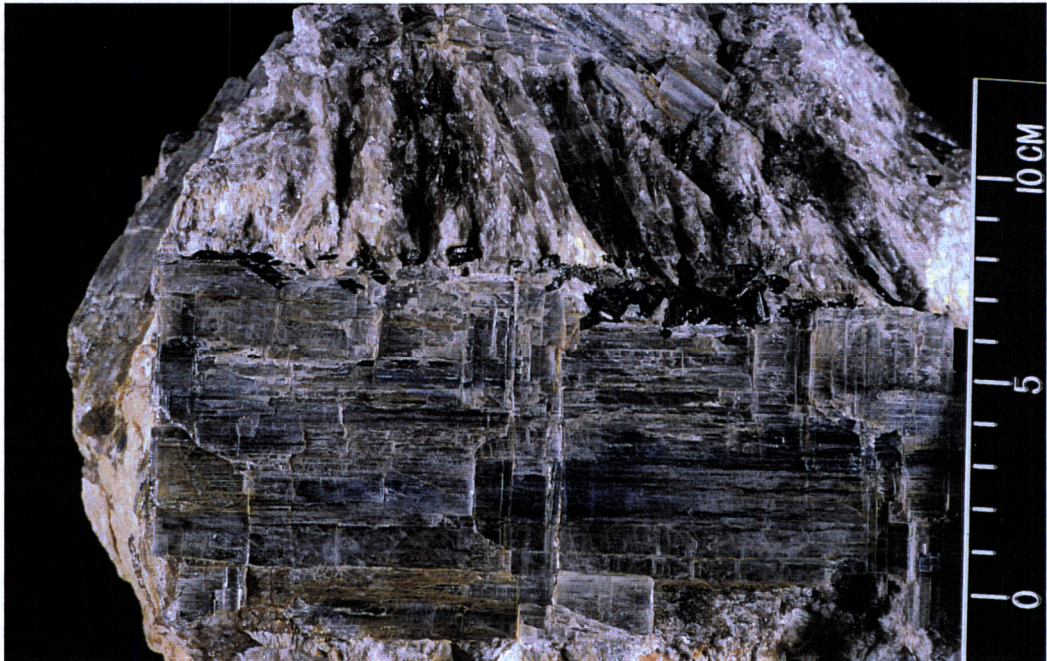


Fig. 5c: Giant kyanite crystal surrounded by plagioclase (bottom of photo) and clustered tourmaline crystals and glassy quartz (center). Dark marks in the kyanite are patchy dark blue color zones. Toward the top of the photo, the end of another kyanite crystal, reported by the original collector to be 70cm long, is visible.



ranges from black to dark brown. Graphic intergrowths of tourmaline and quartz are common. Kyanite is sparsely distributed, being much less common than tourmaline. Other minerals observed include rare garnet and a few tiny zircons. Wallrock alteration appears to have been much less extensive than at the Thomas mine although the host rocks are very similar.

The Meeper mine, located 1.6 km north of the Thomas mine, is the largest of the pegmatites. It is arcuate in shape and approximately 25 m long by approximately 4 m wide. It intrudes rocks similar to those of the other two deposits with the exception that garnet is also present in some of the *unaltered* country rock. Quartz and plagioclase dominate the pegmatite assemblage, followed by roughly equal proportions of biotite and muscovite. Kyanite is slightly less abundant than at the Thomas mine, but crystals reach similar large sizes. Kyanite colors are similar to those reported for the Thomas mine. Tourmaline is scarce here and occurs as small anhedral to subhedral crystals. Garnet within the leucocratic rocks is more abundant here than at the other sites. A few euhedral monazite and xenotime crystals up to nearly 1 cm have been observed. Wallrock alteration seems to have been less intense than at the Thomas mine. Late shearing has broken and bent many of the kyanite crystals and caused surfaces of the crystals to be altered to muscovite.

Samples of the Thomas pegmatite, its wallrocks, unaltered country rock and nearby kyanite- and sillimanite-bearing schists were collected. Mineral and rock samples collected from the pegmatite include representative samples of all minerals across and along the entire exposure. All samples were collected from known locations within the pegmatite, with the exception that samples representing the core and the more distal wallrock assemblages were collected from float that clearly represented those rocks. Analytical methods

used include thin section petrography, quantitative microprobe analyses, XRF whole rock and trace element analyses, and fluid inclusion microthermometry.

Petrography

Pelitic schist near the Thomas mine contains kyanite, muscovite, biotite, garnet, quartz, plagioclase, ilmenite-rutile intergrowths, as well as minor apatite, monazite, and sillimanite as finely dispersed needles and clumps of fibrolite. No evidence of significant shearing or extensive retrogradation was observed. Garnets in these rocks are typically euhedral.

The ultramafic rocks hosting the Thomas mine consist of weakly foliated needles of hornblende and poikiloblastic orthopyroxene. Spinel occurs as clusters of green grains partly surrounding hornblende crystals. Olivine occurs as inclusions in orthopyroxene but is found as isolated grains as well. Chlorite exists as long slender crystals with flat, apparently uncorroded surfaces. Ilmenite, pyrrhotite, chalcopyrite, and pentlandite occur in minor amounts finely distributed through the rock.

Quartz from all zones of the pegmatite contains abundant, long, microscopic needles of sillimanite with no obvious preferred orientation. The sillimanite crystals average about one micron in width but can be extremely long, having aspect ratios greater than 25:1, and are commonly well terminated with wedge or chisel points.

Chemical Analyses

Whole rock and trace element analyses were conducted on a Philips model 1480 energy dispersive (EDS) X-ray fluorescence (XRF) spectrometer at the Department of Mineral Sciences at the Smithsonian Institution, using a scandium-molybdenum X-ray tube. Operating conditions for whole rock analyses were 40 kV and 60 mA whereas those for trace elements were 80 kV and 30 mA. USGS standard rock powders and synthetically prepared standards were used for calibration. Samples for trace element analysis were hand picked, washed, and ground to minus 200 mesh in a shatterbox using an alumina cup. Unweathered whole-rock samples were prepared by crushing in jaw and roll crushers, splitting the sample, then grinding the resulting split to minus 200-mesh in a shatterbox using an alumina cup. To insure a representative sample the starting whole rock sample size was in all cases greater than ten times the linear dimension of the largest crystal in the rock.

Electron microprobe analyses were conducted using a Cameca SX50 equipped with wavelength dispersive spectrometers (WDS) and a continuous acquisition EDS detector. Quantitative analyses were conducted using the WDS capability of the microprobe, whereas EDS was used only in phase identification. Silicate and oxide standards were used as appropriate. Where grain size permitted, the electron beam was defocused to a 10 by 10 micron raster to reduce volatilization of light elements such as sodium. Data were reduced using the PAP (Pouchou and Pichoir 1985) microanalysis data reduction procedure.

XRF Data

Trace-element analyses were conducted on biotite and kyanite collected from one border to the other in the well-developed southern portion of the pegmatite. A muscovite presumed to be from the core of the pegmatite was also analyzed. Trace element data are presented in Table 1. Biotites nearer the walls are enriched in chromium, vanadium, and nickel relative to those closer to the core, whereas copper, barium, niobium, gallium, thallium, and tin show the reverse trend, being most enriched in samples nearer the core. The muscovite sample had trace element levels largely compatible with these trends. Aquamarine-colored kyanite from near the wall showed high levels of chromium (673 ppm), whereas progressively more weakly colored kyanites nearer the core contain lower amounts of chromium (as low as 22 ppm). Kyanite also showed some enrichment in copper closer to the core. No obvious trends were observed for other elements in kyanite.

Major element chemistry was determined for the unaltered country rock, garnet-hornblende wallrocks with minor biotite, and garnet-biotite wallrocks. Trace element levels were also determined for the unaltered country rock. Results of the major element analyses are presented in Table 2 and the trace element analysis of the country rock is given with the other trace element analyses in Table 1. The country rock and garnet hornblende samples were recovered from float that was clearly a product of previous mining. The garnet plus biotite sample was collected *in situ* within a few centimeters of the leucocratic rocks and contained minor quartz and plagioclase. The data show silica and potassium increasing toward the pegmatite, whereas iron decreases.

Table 1. Trace element analyses.

PPM	M1	M2	M3	M4	M5	M6	M7	M8	M9	M10	KY1	KY2	KY3	CR
Rb	409	400	459	454	435	244	463	487	374	388	7	6	6	0
Cs	0	0	0	0	0	1	0	0	10	23	0	0	0	0
Ba	794	1457	2071	2820	3344	6152	1717	1413	558	1565	2	0	0	0
Sr	7	19	4	0	6	54	10	4	34	6	2	2	1	6
Ga	50	61	71	77	71	94	77	66	70	74	45	39	56	14
Tl	11	15	18	18	17	25	20	13	17	19	7	7	11	0
Pb	9	24	42	24	26	114	49	40	93	0	18	33	9	10
Nb	8	46	61	85	102	115	73	48	71	24	4	4	3	2
Ta	12	10	14	10	26	8	13	11	9	3	6	10	8	0
Y	5	25	6	6	18	2	19	7	3	5	9	1	1	68
V	244	150	120	83	133	75	142	179	5	125	80	79	31	150
Ni	475	461	313	307	315	21	423	438	1	433	19	19	8	829
Zn	348	474	577	508	549	77	516	596	97	310	6	2	2	72
Zr	9	67	7	6	11	11	78	39	6	9	15	2	0	59
Sn	16	19	67	54	61	79	56	39	97	24	0	0	4	25
Cr	836	325	168	11	43	0	423	519	5	455	673	367	22	1798
W	0	0	0	0	0	39	0	0	9	0	3	0	2	1
Cu	22	28	29	34	30	27	32	26	0	26	55	65	101	112

M1-M5, and M7-M8: Thomas Mine biotite samples from known locations in the pegmatite, as shown in Fig. 8.

M6: Muscovite from Thomas Mine core float.

M9: Muscovite from Swan Prospect.

M10: Biotite from Meeper Mine.

KY1-KY2: Thomas Mine kyanite samples from known locations in the pegmatite, as shown in Fig. 8.

KY3: Kyanite from Thomas Mine inner zone float.

CR: Unaltered Thomas Mine host rock.

Table 2. Whole-rock analyses

WT %	1	2	3
SiO ₂	51.82	44.51	42.84
TiO ₂	1.11	1.16	0.72
Al ₂ O ₃	17.20	19.99	13.10
Fe ₂ O ₃	9.54	12.18	12.58
MgO	11.33	10.77	22.51
CaO	0.79	9.88	7.12
MnO	0.59	0.31	0.17
P ₂ O ₅	0.04	0.09	0.07
Cr ₂ O ₃	0.04	0.04	0.23
NiO	0.04	0.03	0.17
K ₂ O	4.75	0.20	0.07
Na ₂ O	0.41	1.08	0.14
LOI	2.53	0.78	1.33
Total:	100.19	101.02	101.05

- 1: Garnet+biotite sample UH-B9-GBT collected from east margin, south end, Thomas Mine.
- 2: Garnet+hornblende+minor biotite wallrock sample GT-HBL collected from float at Thomas Mine.
- 3: Olivine-bearing, spinel, orthopyroxene, hornblende schist; sample PCR-UH representing fresh unaltered Thomas Mine host rock.

Microprobe Data

Representative analyses of some wallrock and pegmatite minerals are given in Table 3. The data indicate that plagioclase from the transitional garnet-hornblende-biotite wallrocks is variable in composition but always calcic, averaging An₇₄, whereas plagioclase from the biotite-gedrite-cummingtonite rocks nearer to the pegmatite is less calcic, averaging An₅₂. Pegmatite plagioclase compositions cluster tightly around An₃₄. Similarly, garnet from the transitional rocks contains unusually high calcic (10-13 mol% grossular) and magnesian (29-33 mol% pyrope) components. Garnet from glassy quartz in the outer zone of the pegmatite is lower in calcium, iron, and magnesium, and substantially higher in manganese (21 mol% spessartine.)

Fluid Inclusions

Fluid inclusions were studied to help constrain the P-T conditions of formation of the Thomas Mine rocks and the nature of fluids interacting with them. All fluid inclusions studied were single phase at room temperature (Tr). These inclusions occurred along healed fractures in glassy inner zone quartz. No primary fluid inclusions were observed, nor was any evidence of decrepitation or necking-down detected (Vityk and Bodnar 1995). Inclusions range in shape from ratty to perfect negative crystals although shapes are consistent along any given fluid inclusion assemblage (FIA) (Goldstein & Reynolds 1994). Healed fractures containing ratty to euhedral inclusions were observed crosscutting fine sillimanite needles in the quartz and where this occurred the sillimanite was partly corroded.

Table 3. Microprobe analyses of minerals from altered wallrocks and pegmatite at the Thomas mine.

Wt %	1	2	3	4	5	6	7
SiO ₂	55.71	48.40	54.88	56.79	39.13	39.65	39.10
TiO ₂	0.07	0.27	0.00	0.08	0.00	0.12	2.13
Al ₂ O ₃	2.44	13.14	28.84	27.89	22.10	22.05	17.42
Cr ₂ O ₃	0.06	0.07	0.07	0.00	0.02	0.09	0.06
MgO	23.27	19.61	0.01	0.01	7.89	9.09	16.23
CaO	0.32	0.50	12.17	10.17	4.96	3.80	0.00
MnO	0.39	0.44	0.00	0.08	2.80	1.53	0.08
FeO	16.35	15.27	0.21	0.04	24.86	25.91	12.28
Na ₂ O	0.15	1.20	5.01	6.02	0.00	0.00	0.40
K ₂ O	0.00	0.01	0.03	0.03	0.00	0.00	8.23
Total:	98.76	98.91	101.22	101.11	101.76	102.24	95.93

Wt %	8	9	10	11	12	13	14
SiO ₂	46.61	48.54	51.49	37.91	38.48	59.45	37.20
TiO ₂	0.61	0.12	0.00	0.03	0.04	n.a.	0.28
Al ₂ O ₃	14.00	32.49	30.40	62.55	22.66	25.41	34.90
Cr ₂ O ₃	0.05	0.00	0.00	0.04	n.a.	n.a.	n.a.
MgO	13.51	0.01	0.02	0.03	6.04	0.00	6.59
CaO	11.42	16.42	13.91	0.01	2.94	7.28	0.22
MnO	0.37	0.02	0.02	0.00	9.89	0.01	0.13
FeO	9.86	0.05	0.04	0.09	22.43	0.00	5.55
Na ₂ O	1.34	2.27	3.59	0.00	0.00	7.71	2.08
K ₂ O	0.36	0.03	0.03	0.00	0.00	0.19	0.01
Total:	98.13	99.95	99.50	100.66	102.48	100.05	86.95

1: Cummingtonite from biotite-gedrite-cummingtonite wallrocks.

2: Gedrite from biotite-gedrite-cummingtonite wallrocks.

3-4: Plagioclases from biotite-gedrite-cummingtonite wallrocks. Most calcic and least calcic analyses shown, respectively.

5-6: Garnets from garnet-biotite-hornblende transitional wallrocks.

7: Biotite from garnet-biotite-hornblende transitional wallrocks.

8: Hornblende from garnet-biotite-hornblende transitional wallrocks.

9-10: Plagioclases from garnet-biotite-hornblende transitional wallrocks.

Most calcic and least calcic analyses shown, respectively.

11: Sillimanite needle included in pegmatite core quartz.

12: Garnet from glassy quartz area exposed in south end of pegmatite.

13: Plagioclase from south end of pegmatite.

14: Tourmaline, presumed to be from core; loose crystal collected from float.

Table 3 Continued

Wt %	15	16	17	18	19	20
SiO ₂	53.12	53.41	38.07	29.39	0.00	0.04
TiO ₂	0.37	0.03	0.02	0.15	54.96	0.02
Al ₂ O ₃	7.21	2.62	0.04	22.06	0.01	64.99
Cr ₂ O ₃	n.a.	n.a.	n.a.	n.a.	0.02	1.73
MgO	19.95	29.70	40.46	29.47	4.06	14.42
CaO	12.18	0.27	0.01	0.01	n.a.	n.a.
MnO	0.07	0.26	0.31	0.07	0.68	0.11
FeO	5.46	13.57	21.30	6.10	40.18	17.70
ZnO	n.a.	n.a.	n.a.	n.a.	0.05	0.16
Na ₂ O	0.37	0.00	0.01	0.05	n.a.	n.a.
K ₂ O	0.09	0.01	0.02	0.01	n.a.	n.a.
Total:	98.82	99.86	100.23	87.31	99.95	99.16

- 15: Hornblende.
- 16: Orthopyroxene
- 17: Olivine
- 18: Chlorite
- 19: Ilmenite
- 20: Spinel

One hundred eight inclusions were examined using a gas-flow heating and cooling stage. Melting temperatures (T_m) of CO_2 ranged from -62 to -58 °C and homogenization (T_h) to the liquid phase ranged from -60 to 7 °C. Results are presented as a T_m - T_h diagram in Figure 6. Inclusions with the lowest T_h (highest density) have negative crystal shapes, whereas the shapes grow progressively more ratty with higher T_h . Melting temperatures indicate the inclusions are CO_2 -rich. Laser Raman Spectroscopy showed that small amounts of N_2 are present, and are probably responsible for depression of the freezing point. X_{CO_2} is estimated to be .90. Based on van den Kerkhof's (1990) data, this range in T_h corresponds to densities in the CO_2 - N_2 system of approximately 40 to 60 cm^3/mol .

Discussion

Selected trace element data for biotite are presented in Figure 7. Figure 8 shows the location in the pegmatite from which each biotite was taken; the muscovite sample represents the core of the pegmatite and was collected from float. The order in which the analyses are presented is the same in each graph, although the order does not correspond strictly with a linear traverse of the pegmatite because biotite was not ubiquitous. The analyses are arranged according to the relative distance of the samples from the wallrocks. Interpreted in this way, the trace element data are consistent with a magmatic fractionation process. No other known mechanism could produce the systematic variations observed. The elements chromium, vanadium, zinc, copper, and nickel were probably derived from spinel, pentlandite, and chalcopyrite in the wallrocks. Trace element levels for these metals in the

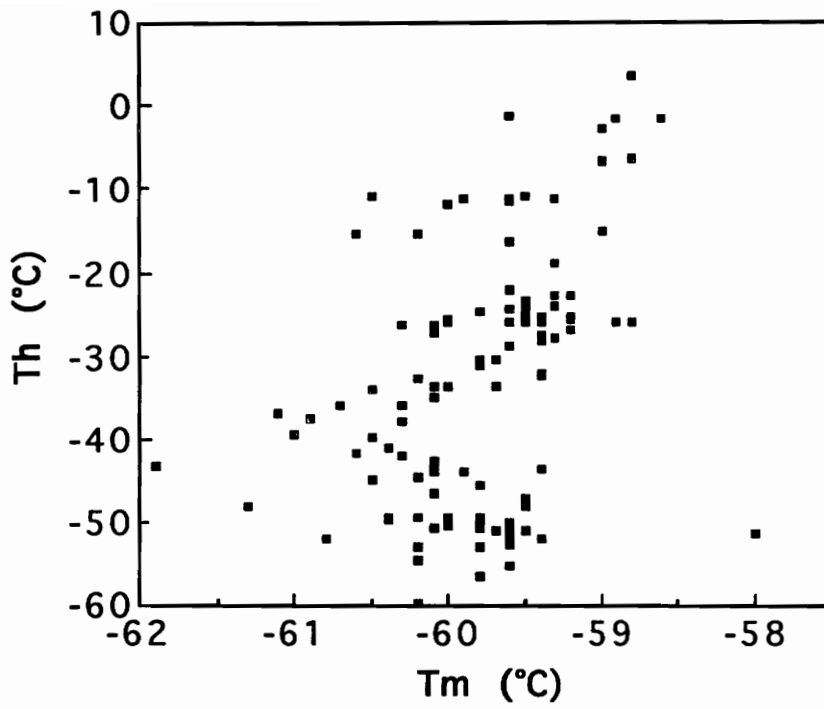


Fig. 6. Th-Tm diagram showing data for 108 CO₂ fluid inclusions in core quartz sample QBB. Homogenization was to the liquid phase.

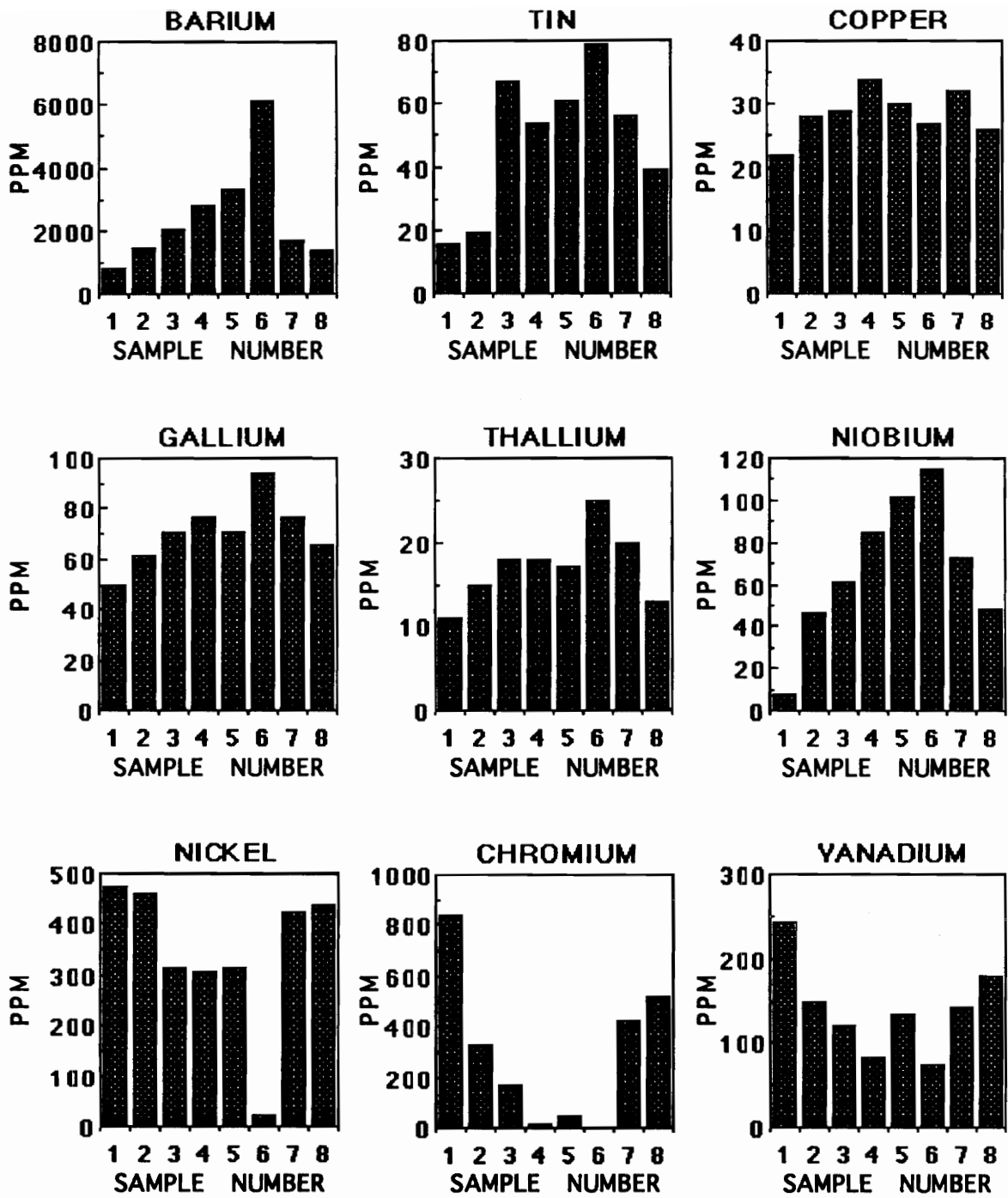


Fig. 7. Trace element concentrations in micas from the Thomas Mine. Numbers 1-8 correspond to micas M1-M8 as reported in Table 1. Number 6 is a core muscovite. Locations in the pegmatite from which samples were taken are shown in Fig. 8. Barium, tin, copper, gallium, thallium, and niobium show higher levels near the core of the pegmatite, whereas nickel, chromium, and vanadium show the reverse trends, being most concentrated in micas toward the walls.

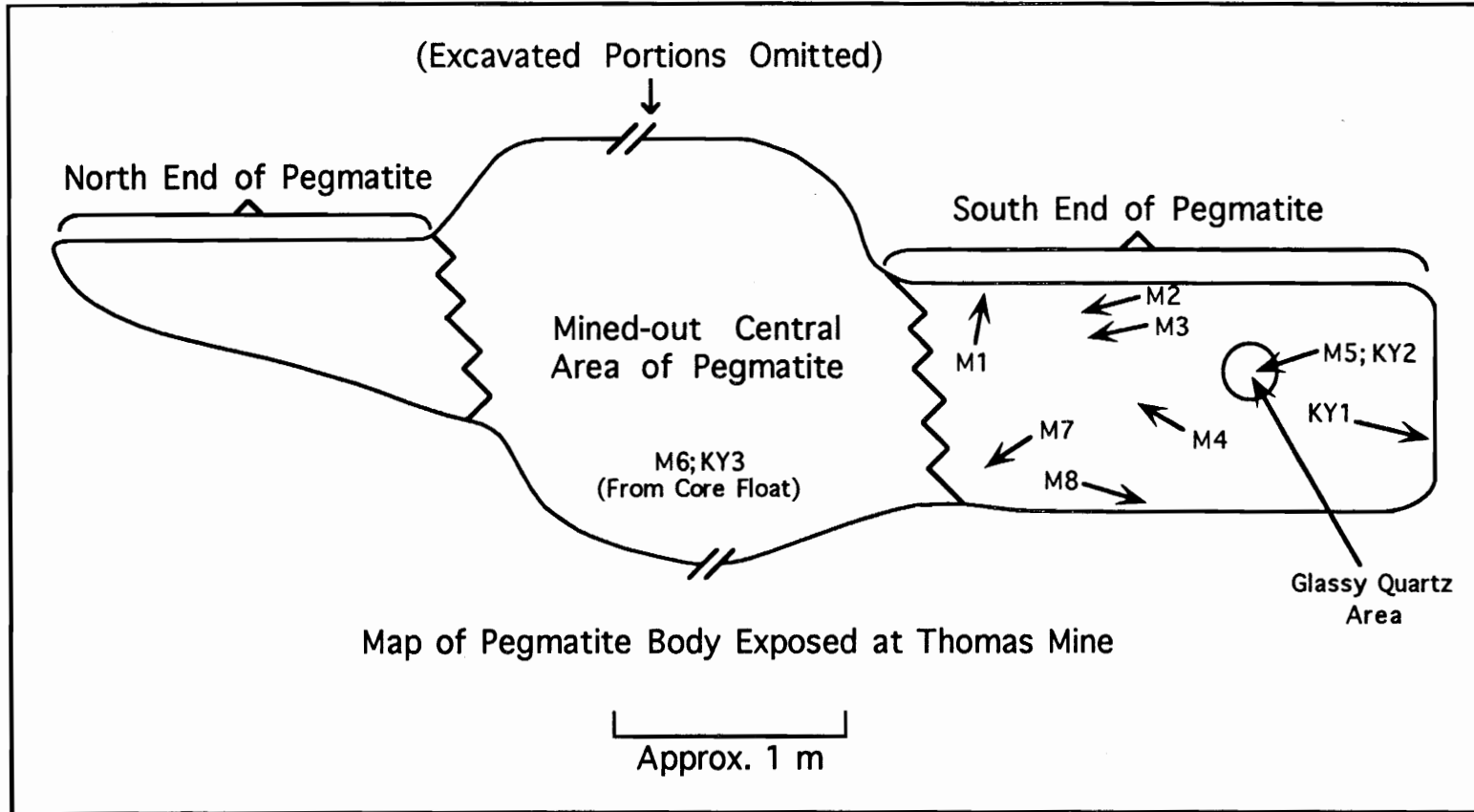


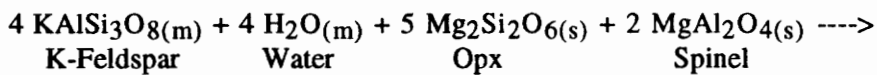
Fig. 8. Cartoon map of pegmatite showing the relative sizes of the north and south ends, the previously excavated central portion, and the locations from which mica and kyanite samples were collected. The glassy quartz area is also indicated. Mineral sample locations are indicated by the tips of the arrows.

pristine country rock (Table 1, analysis CR) suggest that the host rocks were the source. Apart from these metals, only barium is present in significant quantities as a trace element and this can be explained by fractionation. Otherwise the pegmatite shows low levels of virtually all other analyzed trace elements, a fact that is easily understood if the original magma was typical for the simple pegmatites of the Buncombe district (Lesure 1968).

Trace element analyses of kyanite showed clear trends only for chromium and copper. Three kyanite samples were analyzed. Two of these, whose locations are also shown in Figure 8, were from the outer zone, whereas the third sample represented the core of the pegmatite and was taken from float. Chromium levels in kyanite drop dramatically toward the core and correspond with an obvious color difference in the kyanite, probably indicating that chromium, acting as the chromophore, is responsible for the aquamarine color of the kyanite. Kyanite crystals from nearer the pegmatite core show slight enrichment in copper, a factor that may be associated with a very pale green tint seen in some kyanite. These trends strengthen the case for fractionation established by the mica analyses. Additionally, the chromophoric nature of chromium in kyanite can serve as a useful indicator of fractionation extent in future studies, much as the colors of beryl are used in interpreting other pegmatites.

The large amount of biotite present at the Thomas mine clearly indicates that significant potassium was introduced into the area during the formation of these rocks. It is probable that a melt similar to those that produced other pegmatites of the Buncombe District intruded the hornblendite at the Thomas Mine. Lesure (1968) reported that plagioclase is the main feldspar of Buncombe district pegmatites, although the rocks usually contain two

feldspars and accessory muscovite. The potassium-bearing melt was clearly out of equilibrium with the hornblende with respect to concentrations of both silica and alkalis, and probably other components as well. As a consequence of this, most of the potassium from the melt appears to have reacted with the wallrocks to produce biotite. It appears that due to the mildly aluminous nature of the host rocks, not all of the alumina from the melt was involved in the production of the biotite. The biotite could have been produced by a reaction such as the following (components in the melt are marked with an *m* and solid phases are denoted with an *s*):

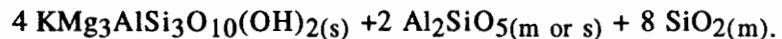


K-Feldspar

Water

Opx

Spinel



Biotite

Kyanite

Quartz

The net result of this reaction, or one similar to it, is that potassium is removed from the melt, leaving a melt enriched in alumina and silica. Spinel has been included in this example reaction to show that alumina from the host rocks was incorporated into the biotite. However, based on the relatively small amount of kyanite in the pegmatite and the volume of biotite present, some alumina from the melt must also have been involved in the formation of biotite. Nonetheless, the K/Al ratio of components removed from the melt had to be greater than unity for there to be relative enrichment of the melt in alumina. Note that kyanite component as a reaction product is marked as either melt or solid. This has been done because there is textural evidence in the pegmatite that kyanite was the first of the leucocratic phases to form (See paragenesis, Figure 9), indeed, kyanite probably began forming soon after

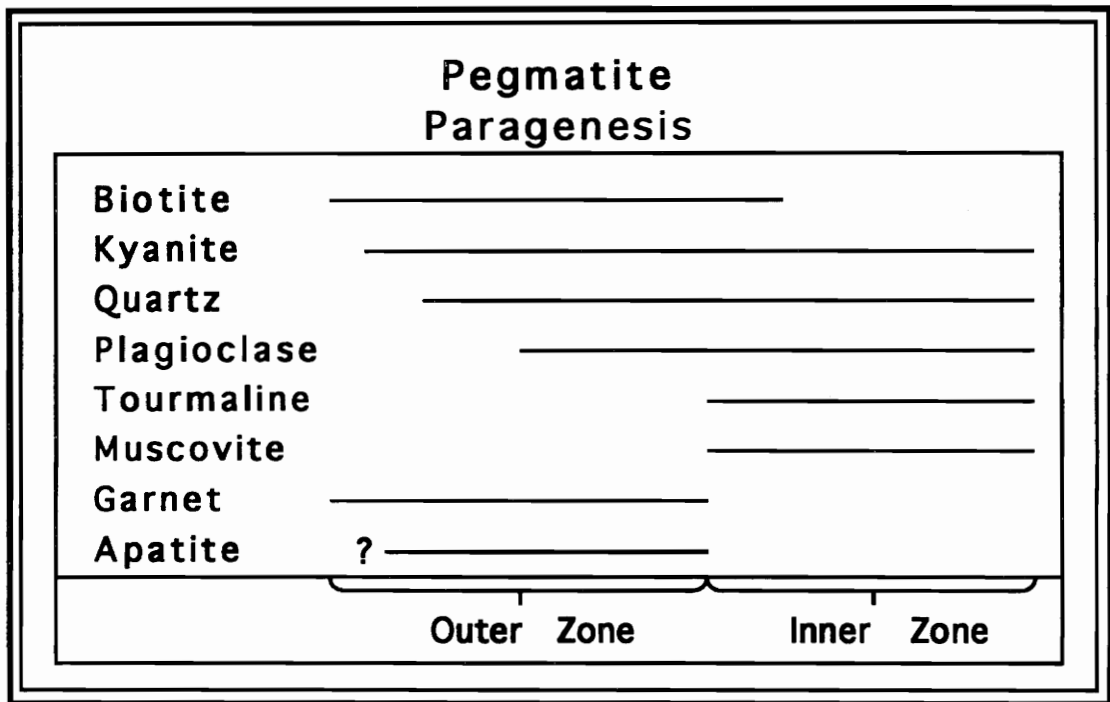


Fig. 9. Paragenesis for minerals occurring in the pegmatite and in the wallrocks closest to it. Biotite began forming almost immediately upon intrusion of magma into the hornblendite, and continued for some time, depleting the melt in potassium. The melt became saturated with aluminum silicate and began crystallizing kyanite. Kyanite formation was followed by nucleation of quartz on still-growing kyanite crystals in the outer zone. Plagioclase followed quartz in the outer zone. Tourmaline, occurring only in the inner zone, formed before quartz, or concurrently with it. Muscovite formation consumed the small amount of potassium remaining in the melt after the wallrocks had been closed off from the melt by crystallization of the outer zone. Garnet, present in large amounts along the pegmatite borders, and sparsely within the pegmatite itself, represents both a melt-wallrock reaction product (Ca-richer) and a pegmatite mineral proper (Mn-richer). The onset of crystallization of subhedral apatite in the wallrocks is difficult to determine. Apatite is absent from the inner zone.

alumina enrichment began, as alumina solubility in granitic melts is very low (Voigt and Joyce 1991). Most kyanite in the outer zone is surrounded by quartz and has modifications to its faces indicating that quartz, probably nucleating on the surfaces of kyanite crystals, was in spatial competition with the kyanite for material from the melt. The ridges separating opposite-facing scallop-shaped depressions visible on kyanite crystals may represent the last portions of the kyanite crystals in contact with the melt before the kyanite was closed off from the melt by the overgrowth and convergence of quartz grains. Thus while potassium from the melt was being extracted by biotite-forming reactions, kyanite may have been simultaneously crystallizing, keeping the melt in a state of continuous saturation in alumina. The ubiquitous, randomly oriented sillimanite needles were probably also crystallizing concurrently. Thermobarometry and fluid inclusion data (discussed below) suggest formation of the pegmatite at conditions near the kyanite-sillimanite boundary. The presence of crosscutting fluid inclusion assemblages and the lack of fibrolite mats and foliated clusters of needles argues against sillimanite being a product of later deformation (Černý and Hawthorne 1982). Many of the longer sillimanite crystals exhibit smoothly curving bends and sharp terminations, suggesting they predate the quartz and were suspended in a liquid before being engulfed by crystallizing quartz.

The smooth euhedral morphology of kyanite crystals in the pegmatite core may be indicating that the process of potassium extraction had gone to completion before the crystallization of quartz and plagioclase began there, indeed before crystallization of the outer zone sealed off the melt from the wallrocks. In this scenario, core kyanites would have completed their crystallization before quartz began forming at the surfaces of the kyanites.

Melt in the outer zone was almost certainly supersaturated with alumina at the onset of quartz crystallization, and the kyanites there were still growing in an aluminosilicate-saturated melt when they were sealed off from the melt by enclosure in quartz. Under this assumption, kyanite in the core simply had more time to crystallize, whereas kyanite crystals in the outer zone were being engulfed by the crystallization of quartz and plagioclase from the walls inward. It is noteworthy that micas are uncommon in the core, supporting the idea that potassium diffusion from the melt to the wallrocks had gone to near completion, but thus not surprising that the main mica found in the core is muscovite.

Although oligoclase tends to be the plagioclase commonly associated with granites responsible for generating muscovite pegmatites (Černý 1982), and is common in the typical North Carolina muscovite pegmatites as well (Olson 1944, P. Wood pers. comm.), the anorthite content (An₃₄) of pegmatite feldspar in this study is unusually high, and may be a result of one or both of the following factors. The biotite of the wallrocks contains on average 8.2 wt % potassium as well as 0.4 wt % sodium as wonesite component. These values for biotite correspond to approximately 6.5 mol % wonesite component in the biotite. Sodium also makes up a little over 1 wt % of the gedrite in the modified wallrocks. Considering the small size of the pegmatite examined (less than 20 m² in cross section), the surface area of the pegmatite with respect to the wallrocks (approximately 20 m of contact in the observed outcrop), and the volume of biotite and gedrite formed, it is feasible that the plagioclase composition in the pegmatite could have been shifted toward anorthite by as much as 10 mol % due to removal of sodium from the melt. Alternatively, it may be considered that biotite formation at the expense of calcic amphibole in

the country rocks would have liberated calcium (Brimhall *et al* 1985) and changed the An content of the melt. It should also be noted that plagioclase associated with the various wallrocks (c.f. Table 3, analyses 3, 4, 9, and 10) is even more calcic than that of the pegmatite, in some cases extremely so. Similarly, wallrock garnets are calcic, indicating that these minerals were probably acting as sinks for calcium released by other reactions. Thus it seems likely that the sodium depletion was more important in affecting the composition of the pegmatite plagioclase, and that calcium liberation was involved only to a limited extent, if at all. The net enrichment in calcium observed in the garnet hornblende wallrocks relative to the unaltered country rock (Table 2, analyses 2 and 3, respectively) gives some credence to the notion that calcium was not highly mobile (Brimhall *et al* 1985).

As has been noted in other cases (Černý 1982), tourmalines mimic the composition of the host rocks. Tourmaline compositions in these rocks correspond to approximately 68 mol% dravite, 32 mol% schorl. The low schorl content imparts the dark reddish brown color to the crystals. The relationship of tourmaline crystallization to that of kyanite is unclear. Tourmaline occurs only in the core and the crystals there are commonly densely clustered around kyanite crystals. Morgan *et al* (1990) showed that BO_3 groups are partially coordinated with aluminum in hydrous alkali aluminosilicate melts. Thus, the close spatial association of tourmaline and kyanite in the core may indicate that boron was liberated to form tourmaline during kyanite crystallization. Supersaturation of the outer zone in alumina at the onset of quartz crystallization would have prevented the nucleation of tourmaline, and boron would have been fractionated into the remaining melt. An alternative explanation is that concentrations of boron in the melt simply did not reach

levels that would support tourmaline crystallization until the outer zone had crystallized to some extent, and that kyanite merely provided a nucleation surface for tourmaline when it did begin to form. Broken tourmaline crystals with quartz in the fractures and common well-formed terminations indicate that tourmaline, like kyanite, formed relatively early, and its presence in feldspar may further indicate its crystallization extended over the duration of core crystallization.

P-T Conditions of Formation

Fluid inclusions and thermobarometry based on microprobe analyses help to constrain the conditions of formation of these rocks. The isochores determined for CO₂ inclusions in core quartz were calculated using Holloway's (1981) ISOCHORE program and are plotted in Figure 10. The highest density inclusions probably represent initial trapping of CO₂-rich fluids that infiltrated the region some time soon after crystallization of the rocks. Their composition is consistent with that of fluids found in other high-grade terranes. The range in isochores corresponding to lower-density inclusions must represent fluids trapped along the cooling path of the rocks. They may be evidence that refracturing of rocks containing CO₂ inclusions of the highest density resulted first in release of CO₂ leading to the formation of an intergranular fluid, and then in subsequent re trapping at lower temperatures and pressures. Poor equilibration of the shapes of lower-density inclusions supports this interpretation.

Peak metamorphism of rocks in the Eastern Blue Ridge is thought to have occurred during the Ordovician Taconic Orogeny, and no other later

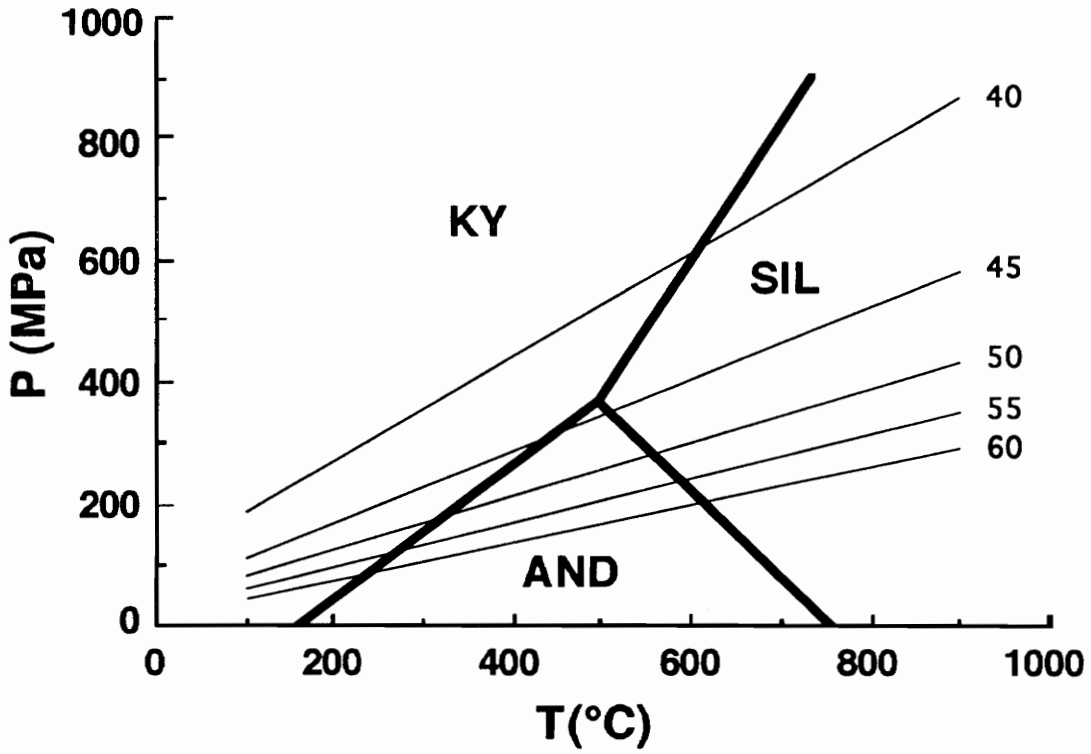


Fig. 10. P-T diagram showing CO₂ isochores calculated using Holloway's (1981) ISOCHORE program. Data from 108 inclusions in core quartz sample QBB. Molar volumes given in cm³/mol are shown next to each isochore.

metamorphic events are believed to have been as intense (Abbott and Raymond 1984). Thus the presence of both sillimanite and kyanite in the pegmatite may be taken as a clear indicator that the pegmatite crystallized at conditions near those of peak metamorphism during the Taconic Orogeny. Consequently, the local high grade metamorphic rocks can shed some light on the conditions of formation of this pegmatite. The mineral assemblage in the nearby kyanite-sillimanite schist permitted the use of the garnet-biotite, garnet-aluminosilicate-quartz-plagioclase (GASP), and garnet-rutile-aluminosilicate-ilmenite (GRAIL) thermobarometers. The mineral analyses used in calculating thermobarometric equilibria are shown in Table 4, and the results of these calculations are presented in Figure 11, which also includes the isochore for the CO₂ inclusions with the highest density from Figure 10.

Additionally, garnet-biotite temperature calculations based on a pressure of 700 MPa were performed on every combination of garnet and biotite possible using 23 biotite analyses and 48 garnet analyses using Ferry and Spear's (1978) original calibration of that system. The 1104 temperatures thus generated have a truncated normal distribution of from 516°C to 736°C. Temperatures below 576°C were discarded on the grounds that they represented garnet-biotite pairs that were far from equilibrium. Remaining 1027 calculated temperatures have a normal bell shaped distribution (Fig. 12). The choice of 576°C as the cut off was to some extent arbitrary, but was chosen because only 77 of the calculated temperatures fell in the 60°C range between 516 and 576°C, and, based on minor chemical zoning within the garnets, they probably represent analyses of garnet formed during a lower-temperature stage of prograde metamorphism. The remaining 1027 calculated temperatures have a mean of 658.6°C and a standard deviation of 29 degrees Celsius. The

Table 4. Representative analyses of minerals in pelitic schist near the Thomas Mine used to calculate thermobarometric equilibria.

WT%	1	2	3	4
SiO ₂	0.01	61.88	38.97	37.07
TiO ₂	52.53	0.00	0.06	2.42
Al ₂ O ₃	0.06	24.51	21.62	19.07
Cr ₂ O ₃	0.01	n.a.	0.00	0.05
MgO	0.18	0.00	4.77	11.30
CaO	0.00	5.63	1.81	0.02
MnO	0.60	n.a.	2.04	0.05
FeO	45.97	0.01	33.70	17.40
Na ₂ O	0.00	8.64	0.04	0.32
K ₂ O	0.01	0.09	0.00	8.51
Total:	99.37	100.77	103.01	96.21

- 1: Ilmenite
- 2: Plagioclase
- 3: Garnet
- 4: Biotite

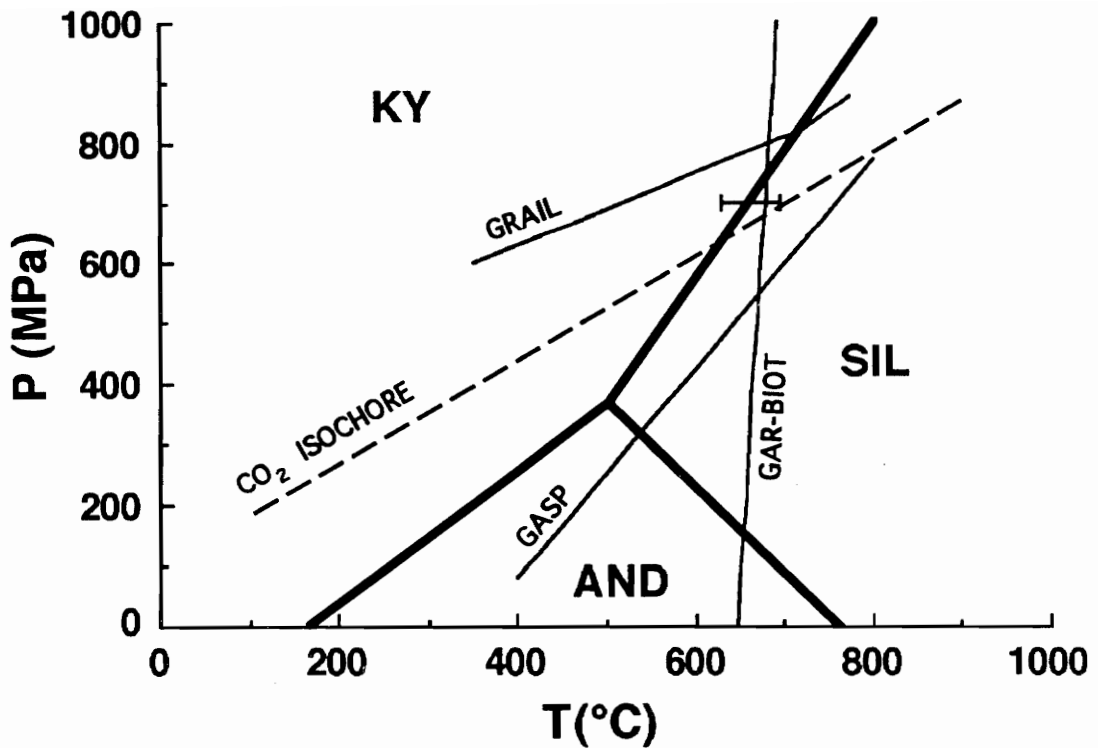


Fig. 11. P-T diagram showing the GASP, GRAIL, and garnet-biotite thermobarometric equilibrium lines calculated for minerals in the kyanite-sillimanite schist near the Thomas Mine. The bracket at 700 MPa shows the temperature range of one standard deviation of the 1027 calculated garnet-biotite temperatures that were above 575°C. Also shown is the CO₂ isochore for the densest fluid inclusions in pegmatite core quartz. The lines converge closely around the kyanite-sillimanite line between 600 and 700°C and 600 to 800 MPa. The coexistence of primary kyanite and sillimanite in the pegmatite constrains conditions of formation further.

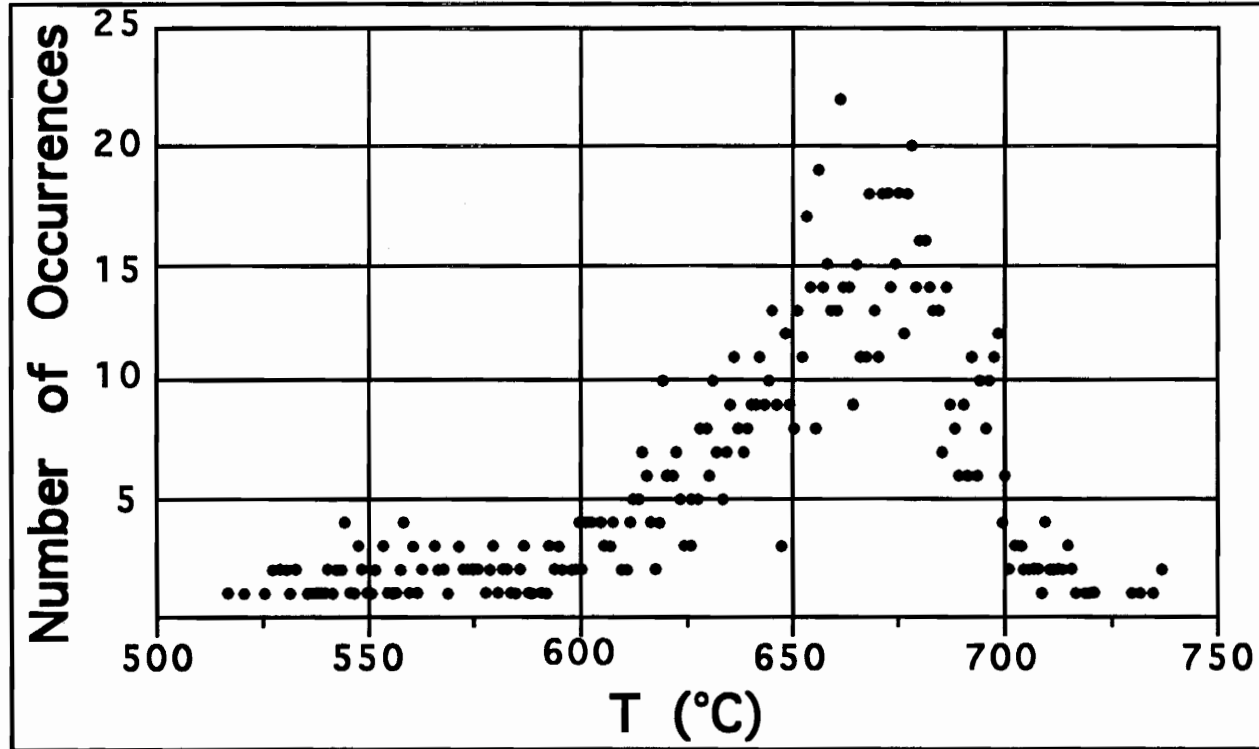


Fig. 12. Distribution of garnet-biotite temperatures calculated from 48 garnet analyses and 23 biotite analyses. The 77 results falling in the range 516-575°C were considered to be too low and too infrequent to be of relevance in determining conditions of formation of the pegmatite. The remaining 1127 results have a normal distribution and a standard deviation of 29°C.

garnet-biotite points plotted in Figure 11 represent the mean temperature of 658.6°C and one standard deviation. As shown in Figure 11, the CO₂ isochore, the garnet-biotite temperature line, and the GASP and GRAIL equilibrium curves all intersect near the kyanite-sillimanite equilibrium curve at approximately 650°C and 700 MPa. Allowing for some error in these methods, it is likely that the pegmatite intruded at conditions of from 600 to 800 MPa and 625 to 675°C, values that are consistent with those of Abbott and Raymond (1984) for metamorphism of the Ashe Metamorphic Suite.

Undercooling by Elevation of the Liquidus

Extraction of the greater portion of potassium from the melt via wallrock interactions raises interesting questions about how this might affect the liquidus of the remaining melt. Discussion of this is best done by first considering a simple system, then evaluating the affect of compositional changes on that system, and finally observing the affect of adding other components to the system. If the original melt prior to extraction of potassium contained equal molecular proportions of quartz and each of the two feldspars, and the plagioclase was An₂₅ (that is, anorthite component made up 8.33 mol % of the melt, excluding water), the melt would have reached the quartz-plagioclase-orthoclase cotectic at approximately 650°C (Winkler 1979, Fig. 18-9). It is probable that either the quartz or plagioclase liquidus would have been reached first at some temperature above 650°C, but, due to the composition being near that of the granite minimum, not higher than perhaps 700°C. The solidus would be 630°C (Winkler 1979, Fig. 18-9).

Removal of some sodium and the majority of the potassium from the melt by wallrock reactions would have had significant effects on the liquidus temperatures discussed above. In the absence of significant potassium the melt is better modeled by the system Ab-An-Qtz-H₂O than by the granitic system used to model the original melt. Yoder's (1968) work in the Ab-An-Qtz-H₂O system at 500 MPa (Fig. 13) suggests that the quartz-plagioclase (An₃₄) cotectic for a water-saturated melt is around 775°C and that, with a melt containing equal proportions of quartz and plagioclase, the quartz liquidus would be intersected first at approximately 800°C. For the same system at 700 MPa this temperature would have been 780°C (c.f. Johannes 1984, Fig. 7). This system is closer to an approximation of the melt after potassium extraction but the model can be improved by considering the addition of excess aluminosilicate. Voigt and Joyce (1991) showed that addition of sillimanite to the system albite-quartz-H₂O at 200 MPa had the effect of lowering the eutectic by 16°C from 752°C to 736°C. The change in the eutectic temperature was caused by a lowering of the quartz liquidus. Although the temperatures they report are not applicable at 700 MPa, the temperature decrease associated with the addition of aluminosilicate may be taken to be roughly the same. Incorporating these data into the melt model here presented has the effect of lowering the liquidus from 780°C to 764°C.

Given a host rock temperature of 650°C (+/-25°C) at the time of intrusion (based on thermobarometry and fluid inclusions), the (still roughly granitic) melt was either already slightly undercooled at emplacement, or rapidly reached such a state. Nonetheless, it was probably sufficiently near its liquidus to prevent extensive crystallization. As soon as wallrock reactions requiring potassium and sodium began, the melt began to shift toward quartz-

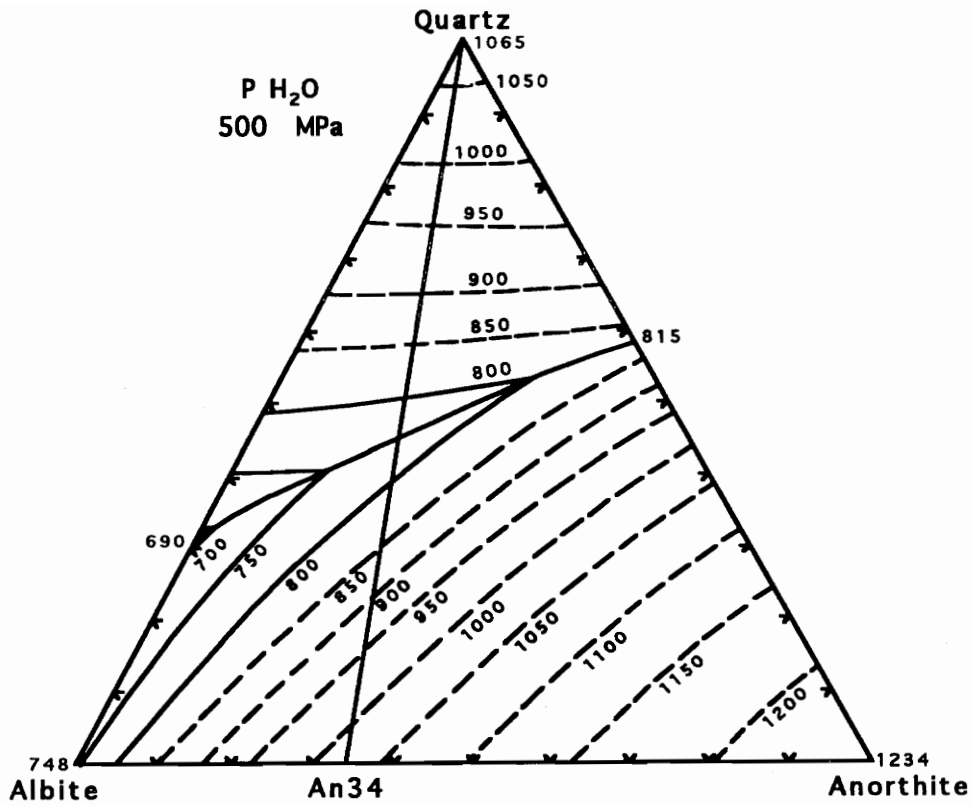


Fig. 13. The Qtz-Ab-An-H₂O quaternary at 500 MPa projected onto the Qtz-Ab-An plane, after Yoder (1968). The intersection of the quartz-An₃₄ pseudobinary and the cotectic occurs at approximately 775°C. For a bulk composition of 50 mol% An₃₄ plagioclase the quartz liquidus is intersected first.

and plagioclase-rich compositions. This was attended by a rise in the liquidus temperatures that was offset only slightly by an increase in aluminosilicate component in the melt. The liquidus of the melt after potassium removal was approximately 764°C, although the melt and country rocks were at 650°C, an undercooling of 114°C. This would lend support to current models of pegmatite formation (London 1992) requiring significant undercooling to account for pegmatitic textures. If the melt was also water-undersaturated, as current models suggest, then the extent of undercooling was even greater than that proposed here, but would be difficult to estimate. In any case, undercooling would have the effect of increasing the viscosity of the melt and hindering nucleation of crystals. Crystals that did nucleate had no obstacles to growth and reached enormous sizes. The uniformity of plagioclase compositions in the pegmatite shows that Ca-Na fractionation was not occurring during feldspar crystallization. This is consistent with a situation in which the chemical potentials of both sodium and calcium were extremely high due to undercooling. If diffusion of sodium and calcium in the melt was slower than the growth of plagioclase crystals then chemical zoning of the feldspar would not develop. However, highly incompatible elements would still be fractionated into the remaining melt, and compatible elements consumed rapidly by growing crystals, giving the trace element patterns observed.

Implications for Muscovite Class Pegmatites

Pegmatites of the Buncombe district tend to have smaller crystals than those found in many pegmatites of the Spruce Pine district, which are also

mineralogically simple. Pegmatites of the Spruce Pine district are thought to be genetically related to granodioritic plutons (Olson 1944, Wood, 1995), and age dates obtained on plutonic and pegmatite samples from that area (S. Goldberg pers. comm.) indicate that those rocks were emplaced at a time equivalent to Acadian orogenic events documented in the Northern Appalachians. The Acadian is a period thought by Abbott and Raymond (1984) to be one of lower grade metamorphism in the Southern Appalachians. The bulk composition of most Spruce Pine pegmatites and that of Buncombe district pegmatites is very similar, but if the Taconic age for Thomas Mine rocks is typical for pegmatites of the Buncombe district then the principle difference between these two groups of pegmatites was the temperature of the host rocks at the time of emplacement. This may be the only factor that explains the textural differences between the pegmatites of the two districts. Pegmatite magmas close in composition to the more granitic magmas discussed above emplaced in very hot country rocks of the Buncombe district would undergo less undercooling than similar magmas intruding the cooler rocks of the Spruce Pine district at a later date. Presumably with less undercooling, nucleation would be less inhibited and grain boundary interference would more readily limit the size of crystals, thus giving Buncombe pegmatites their smaller average grain size relative to those of Spruce Pine. The kyanite-bearing pegmatites of this study underwent greater degrees of undercooling and produced crystals of slightly above average size for the district. Thus, undercooling may be the single most important factor affecting crystallization of magmas lacking significant amounts of network modifiers (London 1992).

Conclusion

The Thomas mine and similar nearby pegmatites in the Eastern Blue Ridge of North Carolina represent the first clearly igneous occurrences of kyanite. The pegmatites formed when small bodies of magma intruded aluminous ultramafic rocks under peak metamorphic conditions of approximately 650°C and 700 MPa. Interaction of the melt with the host rocks resulted in the formation of large amounts of biotite accompanied by a decrease in potassium in the melt. Alumina that was formerly a component of K-feldspar remained in the melt and crystallized to form macroscopic kyanite and microscopic sillimanite. The coexistence of kyanite and sillimanite in the pegmatites and the nearby pelitic schists not only constrains the conditions of formation rather narrowly, but also restricts the time of formation to the Taconic Orogeny of the Ordovician Period. Removal of potassium from the melt caused a change in the position of the liquidus toward higher temperature resulting in *de facto* undercooling, a state that may be of importance in the formation of other muscovite class pegmatites. The coarse crystallinity of the rocks may be attributed to suppression of nucleation due to unfavorable kinetics related to undercooling, and to the extremely high chemical potentials of components remaining in the melt.

References

- Abbott, R.N., & Raymond, L.A. (1984): The Ashe metamorphic suite, northwest north carolina: Metamorphism and observations on geologic history. *Am. J. of Sci.* **284**, 350-375.
- Banerji, A.K. (1954): On a Kaynite pegmatite in Ghadigih, Singhbhum district, Bihar. *Sci. and Culture* **20**, 241-242.
- Brimhall, G.H., Agee, C., and Stoffregen, R. (1985): The Hydrothermal conversion of hornblende to biotite. *Can. Min.* **23**, 369-379.
- Černý, P. (1991): Rare-element granitic pegmatites. Part 1: Anatomy and internal evolution of pegmatite deposits. *Geoscience Canada* **18**, 49-67.
- Černý, P. (1982): Petrogenesis of granitic pegmatites, *in* Granitic pegmatites in science and industry (P. Cerny, ed.). *Mineral. Assoc. Can. Short Course Handbook* **8**, 405-461.
- Černý, P. & Hawthorne, F.C. (1982): Selected peraluminous minerals, *in* Granitic pegmatites in science and industry (P. Cerny, ed.). *Mineral. Assoc. Can. Short Course Handbook* **8**, 163-186.
- Ferry, J.M. & Spear, F.S., (1978): Experimental calibration of the partitioning of Fe and Mg between biotite and garnet. *Contrib. Mineral. Petrol.* **66**, 113-117.
- Goldstein, R.H. & Reynolds, T.J. (1994): Systematics of fluid inclusions in diagenetic minerals. *Soc. for Sed. Geol. Short Course* **31**. SEPM, Tulsa, OK, 199 pp.
- Heinrich, E.W. (1949): Pegmatites of Montana. *Econ. Geol.* **44**, 307-335.
- Heinrich, E.W. (1950): Paragenesis of the rhodolite deposit, Mason's Mountain, North Carolina. *Am. Mineral.* **35**, 764-771.
- Holloway, J.R. (1981): Compositions and volumes of supercritical fluids in the earth's crust, *in* Fluid inclusions: applications to petrology (L. S. Hollister and M. L. Crawford, eds.). *Mineral. Assoc. Can. Short Course Handbook* **6**, 13-38.
- Johannes, W. (1984): Beginning of melting in the system Qz-Or-Ab-An-H₂O. *Contrib. Mineral. Petrol.* **86**, 264-273.
- Keller, F. (1968): Mineralparagenesen und geologie der Campo Tencia-Pizzo Forno-Gebirgsgruppe. *Beitr. Geol. Karte d. Schweiz, N.F* **135**, 72 pp.
- Kerrick, D.M. (1990): The Al₂SiO₅ polymorphs. *Mineral. Soc. of Am. Reviews in Mineral.* **22**, 406pp.

- Kerkhof, A.M. van den (1990): Isochoric phase diagrams in the systems CO₂-CH₄ and CO₂-N₂: Application to fluid inclusions. *Geochim. Cosmochim. Acta* **54**, 621-629.
- Lesure, F.G. (1968): Mica deposits of the Blue Ridge in North Carolina. *U.S. Geological Survey Professional Paper* **577**, 124 pp.
- Lesure, F.G., Grosz, A.E., Williams, B.B., & Gazdik, G.C. (1982): Mineral resources of the Craggy Mountain wilderness study area and extension, Buncombe county, North Carolina. *U.S. Geological Survey Bulletin*. **1515**, 27 pp.
- London, D. (1992): The application of experimental petrology to the genesis and crystallization of granitic pegmatites. *Can. Mineral.* **30**, 499-540.
- Miyashiro, A. (1951): Kyanites in druses in kyanite-quartz-veins from Saihori in the Fukushinzan district, Korea. *Jour. Geological Soc. Japan* **57**, 218-223.
- Morgan, G.B., London, D., & Kirkpatrick, R.J. (1990): Reconnaissance spectroscopic study of hydrous sodium aluminum borosilicate glasses. *Geol. Soc. Am., Abstr. Programs* **22**, A167.
- Nordstrom, C.L. (1947): *Geology of a Kyanite Deposit near Ennis, Montana*. B.S. thesis, Montana School of Mines.
- Olson, J.C. (1944): Economic geology of the Spruce Pine pegmatite district, North Carolina. *North Carolina Dept. Cons. and Devel., Min. Res. Div. Bull.* **43**, 67 pp.
- Pouchou, J.L. & Pichoir (1985): "PAP" Procedure for improved quantitative microanalysis. *Microbeam Anal.* **20**, 104-105.
- Read, H.H. (1932): On Quartz-Kyanite rocks in Unst, Shetland Islands, and their bearing on metamorphic differentiation. *Mineral. Mag.* **23**, 317-328.
- Sanford, R.F., (1982): Growth of ultramafic reaction zones in greenschist to amphibolite facies metamorphism. *Am. J. Sci.* **282**, 543-616
- Sauniac, S., and Touret, J. (1983): Petrology and fluid inclusions of a quartz-kyanite segregation in the main thrust zone of the Himalayas. *Lithos* **16**, 35-45.
- Stuckey, J.L. (1935): Origin of cyanite. *Econ. Geol.* **30**, 444-450.
- Temperley, B.N. (1953): Kyanite in Kenya, with an account of its occurrence in some other countries and a discussion of its origin. *Geological Survey Kenya Memoir* **1**, 87 pp.
- Vityk, M.O., and Bodnar R.J. (1995): Textural evolution of synthetic fluid inclusions in quartz during reequilibration, with applications to tectonic reconstruction. *Contrib. Mineral. Petrol.* **121**, 309-323.

Voigt, D.E. & Joyce, D.B. (1991): Depression of the granite minimum by the addition of sillimanite. *Eos* **72**, p 304.

Winkler, H.G.F. (1979): *The Petrogenesis of metamorphic rocks*. Springer-Verlag, 348 pp.

Wood, P.A. (1995): Petrogenesis of the Spruce Pine pegmatites, North Carolina. *Geol. Soc. Am. Abs. Prog.* **27**, p 468.

Wood, K.Y. (1995): Kyanite-bearing pegmatites in the Blue Ridge of North Carolina. *Geol. Soc. Am. Abs. Prog.* **27**, p 469.

Yoder, H.S. Jr. (1968): Albite-Anorthite-Quartz-Water at 5 KB. *Carnegie Inst., Washington Yearbook* **66**, 477-478.

VITA

Keith Yates Wood was born on January 28, 1964 in Syracuse, New York. Although a childhood interest in minerals was forgotten after a move to Miami, Florida at age eleven, it was rekindled while attending school at Montreat College in western North Carolina. Keith finished a degree in cross-cultural ministry at Montreat in December of 1991, and went on to study geology at Appalachian State University in 1993. There he met his soon-to-be wife and fellow geologist, Patricia Johnson. The two were married during the following summer and immediately moved to Blacksburg, Virginia to begin graduate study in geology at Virginia Tech. An avid mineral collector, Keith's real dream is to strike it rich in some glory hole and retire early on the profits. Barring that, work around rocks would probably suffice.

A handwritten signature in cursive script, appearing to read "Keith Yates Wood".